

for small clusters, the process $\text{Ag}_n \rightarrow \text{Ag}_{n-1} + \text{Ag}$ requires less energy if n is odd, the potentially closed-shell configurations showing more stability.²⁰

The variation of spectral features with pressure (Figure 1) and the supplementary thermodynamic analysis would seem to indicate that we have observed the oxidation of silver clusters. Subsequent experiments are underway to better characterize the silver flux,

to search for the identity of dark products, and to examine the effects of increased agglomeration.

Acknowledgment. J.L.G. acknowledges partial support of this research by the National Science Foundation.

Registry No. Ag, 7440-22-4; O₃, 10028-15-6; AgO, 1301-96-8; Ag₂O, 20667-12-3.

ARTICLES

Kinetics of the NO + CO Reaction on Clean Pt: Steady-State Rates

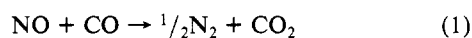
R. L. Klein,[†] S. Schwartz, and L. D. Schmidt*

Department of Chemical Engineering and Materials Science, University of Minnesota, Minneapolis, Minnesota 55455 (Received: February 19, 1985; In Final Form: June 10, 1985)

The kinetics of reaction between NO and CO on clean polycrystalline Pt are studied for temperatures between 300 and 1200 K, pressures between 1 and 10^{-8} torr, compositions from $X_{\text{CO}} = 0.0005$ to 0.99, and rate variations over a factor of 10^8 . Surfaces are shown to be clean before reaction and are found to contain only monolayers of NO or CO following cooling and pumpdown after reaction at any pressure. No nonstoichiometric residues of reactant or contaminant species are observed on the surfaces under any conditions. In excess NO ($X_{\text{CO}} < 0.01$) the steady-state kinetics can be fit quantitatively assuming a Langmuir-Hinshelwood bimolecular rate expression with a heat of adsorption of NO of 17 kcal/mol. For $X_{\text{CO}} > 0.05$, the reaction can be fit by a bimolecular rate expression, $r_{\text{R}} \sim P_{\text{NO}}/P_{\text{CO}}$, at low temperatures, but at high temperatures the rate is proportional to P_{NO} and independent of P_{CO} . Near stoichiometric ratios the reaction appears to be limited by the adsorption rate of NO at high temperatures. For pressures between 10^{-6} and 10^{-8} torr the rate can be fit quantitatively by the same LH mechanism valid at high pressures with a heat of adsorption of CO of 30 kcal/mol. These results strongly suggest that this reaction on Pt is a true bimolecular reaction between adsorbed NO and CO rather than unimolecular NO decomposition with CO scavenging of adsorbed oxygen because the kinetics fit only the former mechanism and because rates are up to 10^4 higher than those of NO decomposition.

Introduction

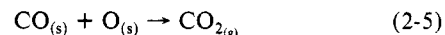
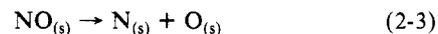
The reaction



over supported Pt, Pd, and Rh is the major reaction of NO removal in the automotive catalytic converter.¹ Reaction in the converter occurs for reactant partial pressures up to 10 torr for widely varying compositions of NO and CO at temperatures up to ~ 800 K. Rhodium is a superior catalyst to Pt, presumably due to its greater ability to dissociate NO.

This reaction has been studied extensively²⁻⁷ on polycrystalline and single-crystal Pt, although no consensus on detailed rate expressions or mechanisms (unimolecular vs. bimolecular rate-limiting steps) has emerged. The (111) plane of Pt is totally unreactive^{2,3} for both unimolecular NO decomposition and the NO + CO reaction under ultrahigh vacuum (UHV) conditions, while the (100) and some high index planes appear to cause complete reaction of the limiting reactant at low coverages.^{3,4}

One mechanism for the NO + CO reaction, proposed by Bell et al.^{8,9} on Pt and other noble metal catalyst surfaces, is a sequence initiated by the dissociation of adsorbed NO, followed by CO scavenging of coadsorbed oxygen which would otherwise poison the surface for further adsorption and reaction. This process would occur through the steps:



Neither CO₂ nor N₂ is believed to chemisorb on Pt although N atoms are observed to be weakly chemisorbed.^{10,11} Therefore, if the rate-limiting step were eq 2-3, the Langmuir-Hinshelwood (LH) rate expression should be

$$r_{\text{R}} = k_{\text{R}}\theta_{\text{NO}} = \frac{k_{\text{R}}K_{\text{NO}}P_{\text{NO}}}{1 + K_{\text{NO}}P_{\text{NO}} + K_{\text{CO}}P_{\text{CO}}} \quad (3)$$

where k_{R} is the surface reaction rate coefficient

$$k_{\text{R}} = k_{0\text{R}} \exp(-E_{\text{R}}/RT) \quad (4)$$

- (1) Taylor, K. C. GM Research Publication GMR 4190 PCP 192.
- (2) Gorte, R. J.; Schmidt, L. D. *Surf. Sci.* **1981**, *111*, 260.
- (3) Gorte, R. J.; Schmidt, L. D.; Gland, J. L. *Surf. Sci.* **1981**, *109*, 367.
- (4) Lesley, M. W.; Schmidt, L. D., to be published.
- (5) Lambert, R. M.; Comrie, C. M. *Surf. Sci.* **1974**, *46*, 61.
- (6) Adlhoj, W.; Lintz, H. G. *Surf. Sci.* **1978**, *78*, 58.
- (7) Singh-Boparai, S. P.; King, D. A. "Proceedings of the 4th International Conference on Solid Surfaces and Third European Conference on Surface Science, Cannes, France, 1980"; Vide, Couches Minces, 1980, No. 201 Suppl.
- (8) Lorimer, P.; Bell, A. T. *J. Catal.* **1979**, *59*, 223.
- (9) Hecker, W. L.; Bell, A. T. *J. Catal.* **1983**, *84*, 200.
- (10) Shigeishi, R. A.; King, D. A. *Surf. Sci.* **1977**, *62*, 379.
- (11) Schwaha, K.; Bechtold, E. *Surf. Sci.* **1977**, *66*, 383.

[†] Present address: UOP, Des Plaines, IL.

and K_{NO} and K_{CO} are adsorption equilibrium constants for NO and CO, respectively

$$K_{\text{NO}} = K_{0,\text{NO}} \exp(E_{\text{NO}}/RT) \quad (5)$$

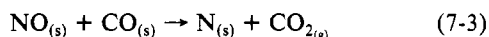
The heats of adsorption of CO and NO, E_{CO} and E_{NO} , under UHV conditions at low coverage are found to be 25–35 and 20–27 kcal/mol, respectively.^{2,3,12} Variations are those between different crystal planes of Pt and for different binding states on each plane.

The unimolecular reaction of NO on clean polycrystalline Pt has recently been characterized in this laboratory for pressures between 0.01 and 1 torr.¹³ It was found that data could be fit quantitatively with a single LH unimolecular rate expression

$$r_{\text{R}} = \frac{k_{\text{R}}K_{\text{NO}}P_{\text{NO}}}{1 + K_{\text{NO}}P_{\text{NO}} + K_{\text{O}_2}P_{\text{O}_2}} \quad (6)$$

with $K_{\text{O}_2} = 8 \times 10^{19}$ molecules/(cm² s) monolayer, $E_{\text{R}} = 13.5$ kcal/mol, $K_{0,\text{NO}} = 7 \times 10^{-4}$ torr⁻¹, $E_{\text{NO}} = 8.2$ kcal/mol, $K_{\text{O}_2} = 1.6$ torr⁻¹, and $E_{\text{O}_2} = 9.6$ kcal/mol. Effective heats of adsorption of NO and O₂ were much lower than those of the tightly bound states on clean Pt, and this was interpreted as reaction through a precursor intermediate.¹²

A surface bimolecular reaction might proceed through the steps



for which the LH rate expression with competitive adsorption and eq 7-3 the rate-limiting step would be

$$r_{\text{R}} = k_{\text{R}}\theta_{\text{NO}}\theta_{\text{CO}} = \frac{k_{\text{R}}K_{\text{NO}}K_{\text{CO}}P_{\text{NO}}P_{\text{CO}}}{(1 + K_{\text{NO}}P_{\text{NO}} + K_{\text{CO}}P_{\text{CO}})^2} \quad (8)$$

The objective of this paper is to characterize the kinetics of NO + CO reaction on clean polycrystalline Pt over a wide range of pressure, temperature, and composition. We shall show that rates measured from 300 to 1200 K and reactant partial pressures from 10⁻⁸ to 1 torr are inconsistent with the unimolecular mechanism and that the rate-limiting step in most situations must therefore be a bimolecular surface reaction between adsorbed NO and CO.

The LH form is, of course, a highly simplified rate expression. It assumes (1) simple crystallographic and adsorption binding state averaging to produce effective *single state parameters*, (2) all processes controlled by *monolayer properties* with no surface or bulk complexes (such as oxide or carbide) which affect rates, and (3) no contaminants, long transients, steady-state multiplicity, or rate oscillations which prevent attainment of *stable steady states*. We are able to eliminate contaminants and demonstrate the absence of surface complexes using a high-pressure cell.¹³ Long transients and oscillations do occur under some conditions, and these will be described in a later paper.¹⁴

Experimental Section

Kinetics and surface characterization were carried out in a system consisting of a small stainless steel reaction cell (~30 cm³) inside a UHV bell-jar system as described previously.¹³ The sample was a 1-cm² ribbon or 0.1-cm² wire of high-purity Pt which could be heated resistively to ~1600 K with temperatures measured by a thermocouple spotwelded to the sample. The sample could be moved by a bellows to position it in front of an Auger spectrometer for AES or seal it in the reaction cell through a Viton o-ring for rate measurements.

The surface was first cleaned by heating to high temperatures in NO or O₂ at ~10⁻⁶ torr until all traces of C, Ca, and S were removed. Once cleaned, contaminants did not return. The cleaned

surface could not be made to form a high-temperature oxide which is associated with Si or Ca contamination.¹⁵ Gases were admitted through stainless steel tubes connected to gas lines through bellows sealed UHV valves. Gases were purified extensively by liquid N₂, activated charcoal, and molecular sieve traps until no contamination (typically C, S, Cl, and Fe) occurred after ~10¹²-langmuir exposures at any surface temperature as shown by AES. TPD spectra also showed NO and CO and their reaction products as the only desorbing gases. This typically required extensive cleaning of inlet lines and traps with baking and UHV pumping.

Pressures up to 10 torr were measured by a capacitance manometer, and partial pressures in the reaction cell were determined by leaking through a variable leak valve to a quadrupole mass spectrometer in the UHV system at ~10⁻⁸ torr. For batch experiments a small constant leak through the Viton o-ring was established by reducing the force on the seal.

Steady-state flow experiments in the reaction cell were made by establishing a known flow rate of a premixed gas mixture by adjusting valves and pumps and measuring rates from partial pressure changes by using the stirred tank equation

$$\Delta P_j = (\tau A T_g / N_0 V) r_{\text{R}} \quad (9)$$

where ΔP_j is the partial pressure change of species j , A the surface area, T_g the gas temperature, N_0 Avogadro's number, and τ the residence time in the cell. The residence time was determined by measuring the rate of pressure decrease from calibrated volumes. The residence time was adjusted between 0.5 and 10 s to maintain the desired conversion during experiments. Mass spectrometer sensitivities were calibrated by using known gas mixtures. Rates measured by this method are regarded as accurate to within 50% on different samples and to within 10% for comparisons on a single sample.

Conversions were maintained below 10% of the limiting reactant where possible so that reactor partial pressures were nearly constant. For high rates and with a large excess of one reactant, conversions exceeded 50% for the shortest measurable residence time. Under these conditions the rate was corrected to that at the inlet pressure after pressure dependences were established. These corrections reduced accuracies near rate maxima to ~30%.

For rates below ~10¹⁵ molecules/(cm² s) the residence time must be inconveniently long to obtain a measurable conversion, and rates were measured by using batch kinetics.¹³ The reaction cell was charged with a known gas mixture, a small leak to the mass spectrometer was established, and the surface was heated to a desired temperature and held constant. The mass balance for species j in a batch reactor is

$$P_j - P_{0j} = (\tau A T_g / N_0 V) \int_0^t r_{\text{R}} dt \quad (10)$$

so the time derivative of the $P(t)$ curve gives the reaction rate at appropriate compositions for a given initial composition. Rates measured by this method are regarded as somewhat more accurate than in the flow situation because complete conversion can be used to calibrate mass spectrometer sensitivities. Most data shown here are from flow reactor measurements although all low rate results were also measured in the batch mode. The batch mode cannot be used above the temperature of the rate maximum because reaction is fast while the temperature is being increased.

It should be noted that in all of these experiments the gas composition is uniform in the chamber because the mixing time (~0.1 s at 1 torr) is much less than the residence time (0.5–10 s) and the characteristic time for reaction. Also, the gas temperature T_g is close to 300 K for any surface temperature because the reactor wall area is much larger than the catalyst surface area.

For rate measurements at pressures between 10⁻⁶ and 10⁻⁸ torr, premixed reactant gases were admitted into the UHV system to the desired pressure with the sample removed from the high-pressure reaction chamber. A poppet valve separating the UHV chamber from the ion and sublimation pumps was partially closed to increase the residence time. This created small but measurable ($\leq 10\%$) partial pressure changes upon heating the sample. The valve also makes pumping speeds for all gases nearly identical

(12) McCabe, R. W.; Schmidt, L. D. *Surf. Sci.* **1977**, *66*, 101.

(13) Mummy, M. J.; Schmidt, L. D. *Surf. Sci.* **1980**, *91*, 301; **1981**, *109*, 29, 43.

(14) Klein, R. L.; Schmidt, L. D., to be published.

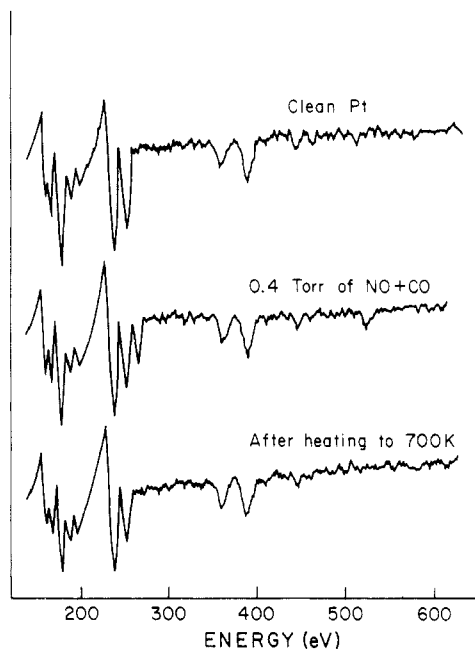


Figure 1. Auger spectra showing clean Pt, after exposure to 0.4 torr of a 1:1 mixture of NO and CO, and after heating this surface to 700 K after pumpdown.

because the residence time is controlled by the orifice through the valve rather than the pumping characteristics for individual gases. In low-pressure measurements the residence time was measured by closing the leak valve and plotting the pressure vs. time semilogarithmically. At low pressures large excesses of one component could not be studied because of contamination from background gases (10^{-10} torr of H_2 and CO).

Results

Surface Coverages. AES spectra were obtained before and after most reaction sequences to assure contamination-free conditions. For all of the rates shown the C, S, and Ca were less than a few percent of monolayer.

Figure 1 shows AES spectra after cleaning, after exposure to an NO-CO mixture at 0.4 torr at room temperature, and after heating to 700 K in the mixture of 0.4 torr. Only C, N, and O are observed, and all of these species disappear upon heating to ~ 1000 K under vacuum. No carbon or oxygen residues were left on the surface in any treatment after sufficient gas purification. Exposure to pure NO at any temperature also did not produce a high-temperature "oxide" on the foil or wire.¹⁵ The N/O and C/O AES peak ratios¹² indicate that 1:1 stoichiometries always occur (nearly equal amounts of N + C and O), and dosing and heating in NO and/or CO up to 1 torr leaves only one monolayer of NO and/or CO after cooling and pumping to 10^{-8} torr. Reaction is therefore inferred to occur only between NO and CO monolayers without involving any multilayer surface complexes.

Nitrous oxide can also be produced by NO + CO reaction. Since both N_2O and CO_2 have major mass peaks at 44, isotopically labeled NO was used to distinguish between these products. The N_2O production rate was found to be no more than a few percent of the N_2 production rate at any temperature even in large excesses of NO. We shall therefore assume that only the N_2 reaction, eq 1, is significant in the reaction between NO and CO.

Excess NO. Below $X_{CO} = 0.01$ (X_{CO} , the mole fraction of CO in the reactant mixture) the low-temperature rate was proportional to P_{CO}/P_{NO} , and above $X_{CO} = 0.05$ the rate was proportional to P_{NO}/P_{CO} . We shall call these regimes "excess NO" and "excess CO", respectively, because these low-temperature kinetics indicate

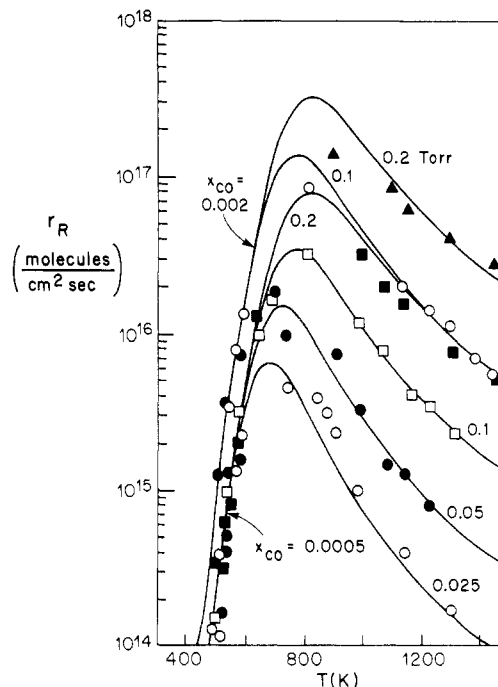


Figure 2. Plot of r_R vs. temperature for $X_{CO} = 0.002$ and 0.0005 for total pressures from 0.025 to 0.2 torr. The curves drawn are from eq 12.

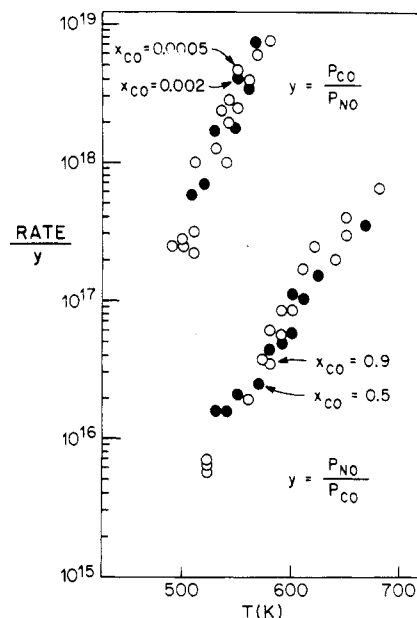


Figure 3. Plot of $r_R(P_{NO}/P_{CO})$ and $r_R(P_{CO}/P_{NO})$ for excess NO and excess CO respectively. All data for each plot lie on a single curve showing that rates have the pressure and temperature dependencies of eq 11 and 13.

that NO is the major surface species below $X_{CO} = 0.01$ while CO is the major surface species above $X_{CO} = 0.05$.

Figure 2 shows r_R vs. T for $X_{CO} = 0.002$ and 0.0005 for several total pressures. All data shown here were obtained using flow conditions. The lack of data points and scatter near the rate maximum occurs because high conversions of CO were unavoidably large and rates had to be corrected to those at the inlet compositions. It is clear, however, that all rates exhibit zeroth-order kinetics in total pressure at low temperature, a maximum at 600–800 K, and a positive order in total pressure at high temperatures.

The low-temperature rate was proportional to P_{CO}/P_{NO} from measurements at all compositions below $X_{CO} < 0.01$. The lower set of data in Figure 3 shows a plot of $r_R P_{CO}/P_{NO}$ vs. temperature for the low-temperature data of Figure 2. Both $X_{CO} = 0.0005$ and 0.002 data fit a single curve when plotted in this manner. The

(15) Niehus, H.; Comsa, G. *Surf. Sci.* **1981**, *102*, 114.

(16) Serri, J. A.; Cardillo, M. J.; Becker, G. E. *J. Chem. Phys.* **1982**, *77*, 2175.

(17) Campbell, C. T.; Ertl, G.; Segner, J. *Surf. Sci.* **1982**, *115*, 309.

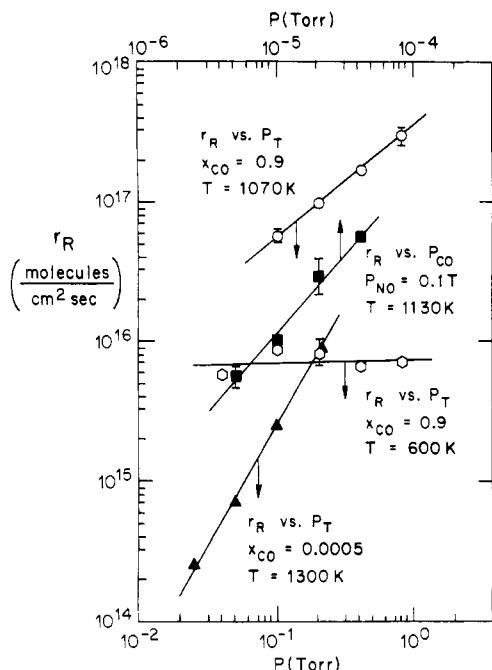


Figure 4. Plots of $\log r_R$ vs. pressures to determine reaction orders in P_{NO} , P_{CO} , and P_T . Values obtained are used in eq 12, 14, and 15.

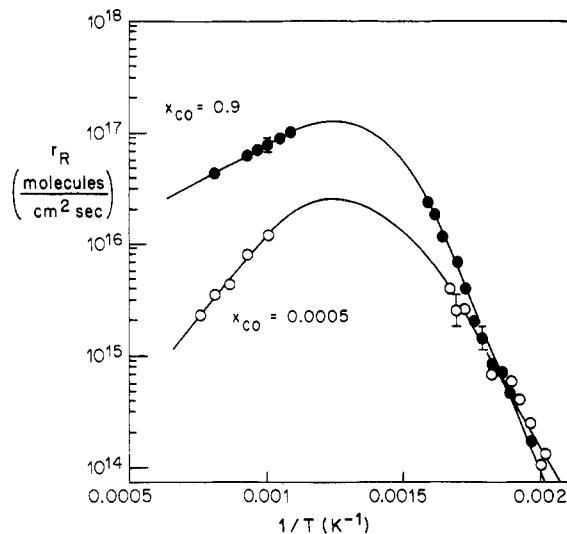


Figure 5. Arrhenius plot to determine reaction activation energies and preexponentials. Values obtained are used in eqs 12, 14, and 15.

slope and intercept show that in excess NO the reaction rate is given by the expression

$$r_R = 1.4 \times 10^{26} \exp(-20400/RT) P_{CO}/P_{NO} \quad (11)$$

with r_R in molecules/(cm² s).

At high temperatures Figure 4 shows that the reaction is first order in P_{CO} and second order overall. The Arrhenius plot of Figure 5 gives the activation energy and preexponential to yield for $T > 1000$ K:

$$r_R = \frac{2.8 \times 10^{18} \exp(13400/RT) P_{NO} P_{CO}}{[1 + (1 \times 10^{-4}) \exp(16900/RT) P_{NO}]^2} \quad (12)$$

The solid curves in Figure 2 are calculated by using this expression.

Excess CO. Above $X_{CO} = 0.01$ the kinetics deviate from the rate expression just described and between $X_{CO} = 0.05$ and 0.99 an expression characteristic of excess CO is valid.

Figure 6 shows r_R vs. temperature for $X_{CO} = 0.5$ and 0.9 for several different pressures. As before, the rates are identical at low temperature for a given reactant composition, indicating zeroth order in total pressure, and, above a maximum at 800–900 K, the rates are positive order in total pressure.

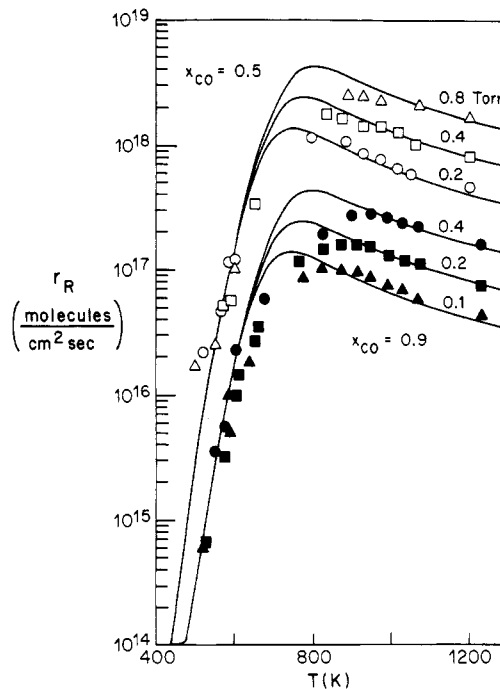


Figure 6. Plot of r_R vs. temperature for $X_{CO} = 0.5$ and 0.9 for pressures from 0.1 to 0.8 torr. Curves shown are from eq 15.

Figure 5 shows low- and high-temperature Arrhenius plots for excess CO, while Figure 3 shows that the rate is proportional to P_{NO}/P_{CO} at low temperatures. Therefore, we find that in excess CO for $T < 700$ K the rate can be fit by the expression

$$r_R = 8.7 \times 10^{25} \exp(-24200/RT) P_{NO}/P_{CO} \quad (13)$$

At high temperatures Figure 4 shows that the rate is first order in total pressure. Examination of Figure 6 shows that r_R is independent of P_{CO} for $T > 1000$ K. Therefore, from pressure and temperature dependences of Figures 3–5 we obtain the expression for $T > 1000$ K.

$$r_R = 3.5 \times 10^{17} \exp(5800/RT) P_{NO} \quad (14)$$

LH rate expression valid at all temperatures for $X_{CO} > 0.05$ is therefore

$$r_R = \frac{3.5 \times 10^{17} \exp(5800/RT) P_{NO}}{1 + (4 \times 10^{-9}) \exp(30000/RT) P_{CO}} \quad (15)$$

The curves shown in Figure 6 are fits to data using eq 15.

Low Pressures. Between 10^{-6} and 10^{-9} torr the reaction rate appeared to attain steady state within a few seconds after establishing the sample temperature. All rates were also found to be identical when a particular temperature was approached from lower or higher temperatures.

The lower half of Figure 7 shows rates with $X_{CO} = 0.5$ for total pressures of 10^{-6} , 10^{-7} and 10^{-8} torr. All rates were obtained with residence times of 1–5 s, and the minimum detectable rate was estimated to be $\sim 10^{10}$ molecules/(cm² s) from the minimum detectable change in the CO₂ signal. Figure 8 shows r_R vs. temperature for $X_{CO} = 0.33$ and 0.67 at the total pressures indicated.

All rates are zeroth order in total pressure at low temperatures and become first order in P_{NO} and zeroth order in P_{CO} at high temperatures. At low temperature the rate is positive order in P_{NO} and negative order in P_{CO} as shown in Figure 8. Therefore, we conclude that the rates of Figures 7 and 8 can be fit accurately by eq 15 in excess CO. It is seen that, while some deviations occur, the rates of low pressure are fit fairly well by the rate expression valid at high pressures.

We attempted to measure the rate of NO decomposition at low pressures without added CO. At 10^{-7} torr no evidence of reaction could be found in that no changes in N_2 , N_2O , or O_2 pressures could be detected upon heating the sample to any temperature. This places an upper bound on the NO decomposition rate of $r_R = 8$

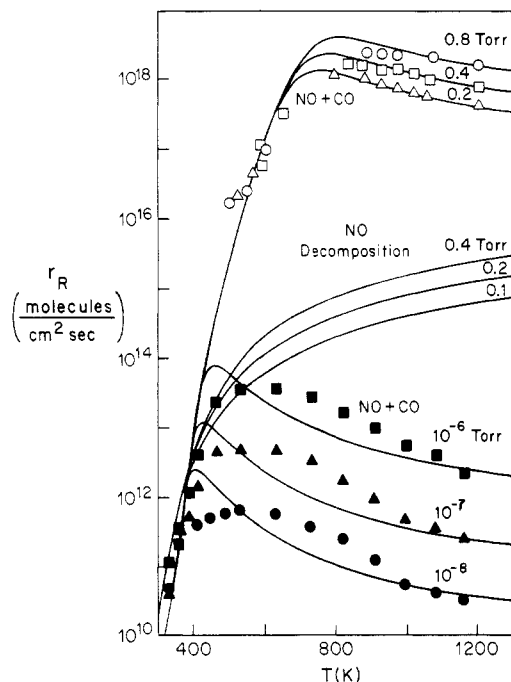


Figure 7. Plot of r_R vs. temperature for equimolar mixtures of NO + CO at 10^{-6} , 10^{-7} , 10^{-8} , 0.2, 0.4, and 0.8 torr and the NO decomposition rate from Mummey et al.¹³ Curves for the NO + CO reaction rate are from eq 15.

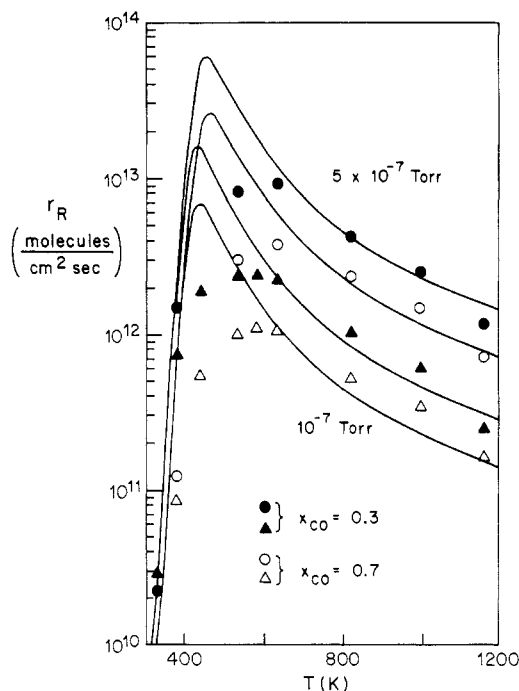


Figure 8. Plot of r_R vs. temperature for 2/1 and 1/2 NO/CO mixtures at 10^{-7} and 5×10^{-7} torr. Curves shown are from eq 15.

$\times 10^9$ molecules / (cm² s) at this pressure.

Discussion

Low vs. High Pressures. A remarkable result of these experiments is that all rates with $X_{CO} > 0.01$ at pressures between 10^{-8} and 1 torr can be fit accurately by a single rate expression, eq 15. This is illustrated in Figure 7, in which sets of data at $X_{CO} = 0.5$ at pressures of 0.8–0.2 and 10^{-6} – 10^{-8} torr are plotted together. The solid curves are from eq 15. No systematic deviations are evident except near the rate maxima.

The high-temperature rates give the order of the reaction to high accuracy. The rate is proportional to P_{NO} to the 1.00 ± 0.01 power. This accuracy is possible because, while measurements

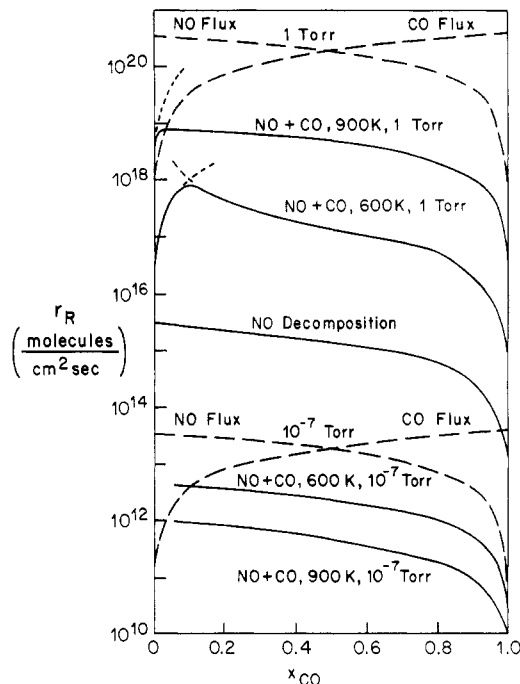


Figure 9. Plot of NO and CO flux rates (dashed curves), equimolar NO + CO reaction rates at 600 and 900 K, and NO decomposition rate at 1 torr and 900 K vs. mole fraction of CO in an NO + CO mixture. Short dashed curves are calculated from the excess NO model and the excess CO model. Upper portion is for $P_T = 1$ torr, lower portion is for $P_T = 10^{-7}$ torr. The NO decomposition rate at 10^{-7} torr is less than 10^{10} molecules/(cm² s) and is not shown.

were made in different reactors (the reaction cell and the UHV system) with independent calibration of parameters, the pressures in the experiments vary by a factor of 10^8 , so that calibration errors are insignificant.

A single curve also fits all low-temperature rate data in excess CO. Note that the temperature of the rate maximum decreases with decreasing pressure as predicted by LH kinetics.

Figure 9 shows a plot of rates vs. X_{CO} at a total pressure of 1 torr (upper portion) and 10^{-7} torr (lower portion). Dashed curves indicate the NO + CO fluxes to the surface at the total pressures. The curves labeled "NO + CO" are calculated from eq 15 at the temperatures indicated and the curve indicated as "NO Decomposition" is from eq 6.

The rising curves at high pressures are for the excess NO expression, eq 12. At low temperatures the rate is predicted to become very high as X_{CO} approaches zero, and the excess NO expression is clearly applicable.

Comparison of reaction rates with gas fluxes gives reaction probabilities (r_R/flux) directly. The reaction probability of the NO + CO reaction is seen to be between 0.1 and 10^{-3} of the limiting species except as X_{CO} approaches zero. The reaction probability of NO decomposition is less than 10^{-5} . As X_{CO} approaches zero, the rate of the NO + CO reaction predicted by eq 12 at 900 K and 1 torr exceeds the CO flux by approximately a factor of 2. The highest pressure for which excess NO rate data was taken was 0.2 torr. At 0.2 torr both the data and eq 12 give a rate below the flux limit. This implies that between 0.2 and 1.0 torr the rate becomes flux-limited in CO.

Unimolecular vs. Bimolecular Reaction. These measurements strongly suggest that the rate-limiting step in the NO + CO reaction is a true bimolecular process, eq 7, rather than the unimolecular NO decomposition step, eq 2. Arguments for this are (1) the rate for $X_{CO} < 0.01$ is fit by a bimolecular LH rate expression and disagrees with the unimolecular reaction and (2) the rate at all compositions is $> 10^3$ higher than that of NO decomposition without CO.

While the form of the rate expression for $X_{CO} > 0.05$ fits that of a unimolecular reaction with CO inhibition at low temperatures, the magnitudes of the rates and shapes of the r_R vs. T curves with

and without CO are quite different. This is illustrated in Figure 7 by the NO decomposition rates at three pressures.

The kinetics of NO decomposition gave excellent agreement with rates predicted by the unimolecular rate expression, eq 6. In those experiments there was no evidence of inhibition by adsorbed oxygen except when O₂ was intentionally added, and no nonstoichiometric species (e.g., atomic oxygen) were detected by AES or TPD following cooling and pumpdown. However, it is possible that NO decomposition at ~1 torr has not been measured without coadsorbed oxygen because in previous experiments the oxygen may have been reacted off the surface before UHV measurements could be made. However, in the present experiments at low pressures AES was used to determine that there was never excess oxygen on the surface during either reaction at $P < 10^{-6}$. The consistency of the NO + CO kinetics between 1 and 10^{-8} torr indicates identical surface conditions in both experiments.

The predicted value of the adsorption equilibrium constant, eq 5, is

$$K_i = \frac{S_0}{\nu_0 n_0 (2mRT_g)^{1/2}} \exp(E_i/RT) = k_0 e^{E_i/RT}$$

where S_0 is the sticking coefficient, K_0 the desorption preexponential factor, and n_0 the monolayer density. If $S_0 = 1$, $\nu_0 = 10^{13}$ s⁻¹, and $N_0 = 10^{15}$ molecules/cm², the preexponential factor K_0 should be 10^{-7} torr⁻¹. Using this relation, one can estimate the temperatures above which various adsorbates should have low coverages ($\theta < 1/2$ when $K_i P_i < 1$) at a particular pressure. Assuming $E = 20, 30,$ and 50 kcal/mol for the most tightly bound states of NO, CO, and O₂, respectively, coverages should be 0.5 at 620, 930, and 1500 K at 1 torr and 330, 500, and 830 K at 10^{-6} torr. Thus, we see that oxygen could be present in sufficient quantities to inhibit NO decomposition below 1500 K at 1 torr but only below 830 K at 10^{-6} torr, while CO could adsorb significantly below 930 and 500 K at these pressures. This calculation ignores competitive adsorption, but the estimates should provide valid upper limits on temperatures. These estimates indicate that oxygen could not be adsorbed significantly on the surfaces in high-temperature experiments at low pressures, and the agreement of kinetics at low and high pressures argues that it is also not present at high pressures. Note also that the temperatures where $\theta_{CO} = 1/2$, 930 K at 1 torr and 500 K at 10^{-6} torr, coincide closely with temperatures of rate maxima as predicted by LH kinetics, eq 3, if CO inhibits the reaction at low temperatures.

Adsorption Limited Reaction. In this section we show that an apparent unimolecular LH reaction eq 3 can be obtained from the bimolecular reaction mechanism, eq 7, if the adsorption step, eq 7-1, is rate limiting. Thus, the reaction could be bimolecular even if the rate expression has the form of eq 3.

The rates of change of θ_{NO} and θ_{CO} from eq 7 are

$$d\theta_{NO}/dt = k_{a,NO}P_{NO}(1 - \theta_{NO} - \theta_{CO}) - k_{d,NO}\theta_{NO} - k_R\theta_{NO}\theta_{CO} = 0 \quad (16)$$

$$d\theta_{CO}/dt = k_{a,CO}P_{CO}(1 - \theta_{NO} - \theta_{CO}) - k_{d,CO}\theta_{CO} - k_R\theta_{NO}\theta_{CO} = 0 \quad (17)$$

The steady-state solutions of these equations can be inserted into $r_R = k_R\theta_{NO}\theta_{CO}$ to give $r_R(P_{NO}, P_{CO})$. It is straightforward to eliminate θ_{NO} and θ_{CO} from these equations, but the expression involves a quadratic equation in pressures which is awkward to solve explicitly. With adsorption-desorption equilibrium k_R is smaller than the k_a 's and k_d 's, and θ 's are given by the Langmuir isotherm which produces the bimolecular LH expression, eq 8.

However, if $k_{d,NO} \ll k_R\theta_{CO}$ and $\theta_{CO} \gg \theta_{NO}$, then from eq 16 and 17

$$\theta_{NO} = \frac{K_{a,NO}P_{NO}(1 - \theta_{CO})}{K_R\theta_{CO}}$$

$$r_R = K_R\theta_{NO}\theta_{CO} = k_{a,NO}P_{NO}(1 - \theta_{CO})$$

Since θ_{CO} is given by a Langmuir isotherm and θ_{NO} is too low for NO competition

$$\theta_{CO} = \frac{K_{CO}P_{CO}}{1 + K_{CO}P_{CO}}$$

$$1 - \theta_{CO} = (1 + K_{CO}P_{CO})^{-1}$$

the reaction rate becomes

$$r_R = \frac{k_{a,NO}P_{NO}}{1 + K_{CO}P_{CO}}$$

This approximation gives the form of a unimolecular NO decomposition reaction with CO inhibition eq 3, except that the adsorption rate coefficients of NO appears in the numerator rather than the quantity $k_R K_{NO}$ predicted by eq 3.

Therefore, we see that the kinetics of the NO + CO reaction are consistent with a single bimolecular rate expression if it is assumed that the adsorption-desorption limit applies when $X_{CO} < 0.01$ and that the adsorption limit applies if $X_{CO} > 0.05$. The major problem with this mechanism is that the only temperature-dependent term in its high-temperature limit $r_R = k_{a,NO}P_{NO}$ is S_0 . Experiments have shown a small temperature dependence of the NO sticking coefficient below 1000 K. This appears to be inconsistent with the decreasing rate of reaction at high temperatures.

We also note that the kinetics in excess NO and excess CO cannot be fit by assuming parallel processes of unimolecular and bimolecular rates

$$r_R = r_{uni} + r_{bi}$$

because in excess CO the bimolecular expression (with parameters obtained from data in excess NO) predicts a rate several orders of magnitude higher than those observed.

Finally, we note that the reaction probability in excess NO (ratio of reaction rate to the flux predicted by gas kinetic theory) exceeds unity using the rate expression valid in excess NO. This is further evidence for an adsorption-limited process in excess CO.

Deviations from Langmuir-Hinshelwood Kinetics. All rates in Figures 2 and 6-8 can be fit accurately by simple LH expressions, eq 12 and 15, except near the rate maxima. We shall develop two simple models that yield better fits to the experimental results and may give a better qualitative understanding of the NO-CO reaction.

The data in Figures 2 and 6-8 deviate from the LH expressions, eq 12 and 15, under conditions where coverages are changing rapidly with T , i.e., near the rate maxima. At temperatures below the maximum, coverages are nearly unity and saturated surface parameters should apply, while at high temperatures the surface is nearly clean and parameters should be those of low coverages.

The heat of adsorption of most chemisorbed species varies strongly with adsorbate coverage. This can be caused by adsorbate-adsorbate interactions or by multiple binding states on a crystal plane or on different crystal planes. In any case, the heat of adsorption E_d can be approximated as $E_d = E_0 - \alpha\theta$ where E_0 is the heat of adsorption at $\theta = 0$ and α is a constant. The adsorption equilibrium constant K_i of eq 5 is then given by the expression

$$K_i = K_{0i} e^{E_0/RT} e^{-\alpha\theta/RT}$$

When this is inserted into eq 15 with $\alpha < 0$ one obtains, after eliminating θ by iteration, a rate vs. temperature curve whose maximum is lowered and broadened as shown in Figure 10. The physical interpretation implied by this expression is that repulsive interactions cause the NO coverage to become low sooner than predicted by LH kinetics.

An alternate explanation of the broad rate maximum comes from an adsorption-limited rate if r_R approaches the flux limit. The bimolecular mechanism gives a quadratic for $r_R(P, T)$ if adsorption-desorption equilibrium is not assumed. The unimolecular mechanism at steady state gives an equilibrium constant K_i in eq 3 (now a steady-state constant) of

$$K_i = k_a/(k_c + k_R)$$

If E_R, E_d , and preexponentials are chosen properly, then $k_R > k_d$

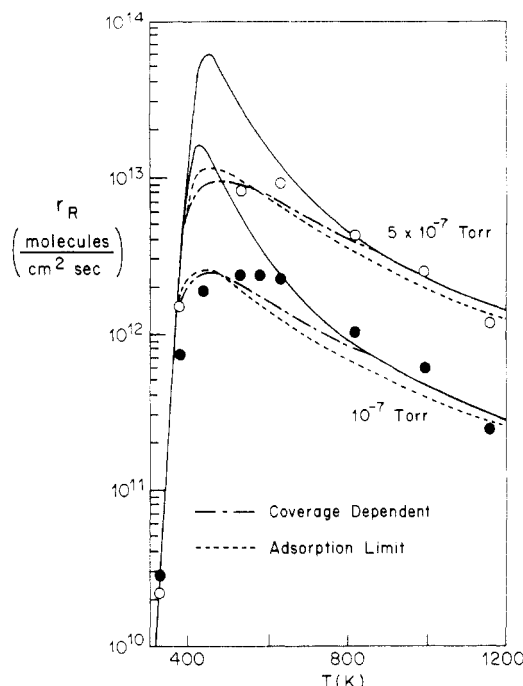


Figure 10. Plot of r_R vs. T for LH model (solid curve) and models with adsorption limit and coverage dependent activation energy. For E_{CO} (θ_{CO}), $\alpha = 12000$ cal/(gmol K) and $E_0 = 42000$ cal/(gmol K). For the adsorption limit, $k_{aNO} = 5 \times 10^{19}$ molecules/(cm² s), $k_R = 7 \times 10^{10} e^{14050/RT}$ s⁻¹, $k_{dNO} = 10^{13} e^{8250/RT}$ s⁻¹ and $k_{CO} = 4 \times 10^{-9} e^{24200/RT}$. Both models predict a lower and broader rate maximum than observed.

at low temperature and $k_R < k_d$ at high temperature. This can give a broad maximum as shown in Figure 10.

We do not claim that either of these mechanisms gives an accurate explanation of rate data, but merely note that they give good fits to data. Models could only be distinguished if extremely accurate adsorption and reaction rate data were available.

Summary

The kinetics of the NO + CO reaction on polycrystalline Pt measured over a wide range of temperatures, pressures, and

compositions can be interpreted accurately using Langmuir-Hinshelwood models. While kinetics cannot prove mechanisms, the agreement with this rate expression indicates that the reaction steps are simple adsorption, desorption, and reaction in coadsorbed monolayers on the surface. AES confirms the absence of excess oxygen, nitrogen, or carbon and eliminates the possibility of contaminants.

Each crystal plane of the Pt surface is known to have characteristic NO and CO adsorption and reaction parameters. This could lead to very complicated kinetics on a polycrystalline catalyst. None of these effects is evident in rate measurements in that LH models give adequate descriptions of data. This of course does not imply that they do not exist but only that the averaging process over crystal planes and binding states does not reveal their presence. In fact, the (111) plane, the lowest free energy and probably most abundant plane of clean polycrystalline Pt, is not reactive at all. The unreactivity of Pt(111) should be evident only in making the preexponential factor of k_R slightly smaller than it would be if the (111) plane were not present.

These results also indicate strongly that the rate-limiting step is a bimolecular reaction step between NO and CO rather than the unimolecular dissociation reaction. The magnitude of the rate and its dependences on temperature and on NO and CO partial pressures appear to be inconsistent with NO dissociation as the rate-limiting step.

The low activity of Pt in the automotive catalytic converter is not simply explained by these results because the rate expression predicts adequate rates of reaction. Presumably, the inhibition by O₂, CO, or other species causes the reduced activity of Pt compared to Rh for NO reactions. Perhaps Rh is a superior catalyst because the dissociation of NO occurs instantly upon adsorption, and therefore the overall reaction does not depend on a true bimolecular process which may more easily be inhibited by other species.

Finally, we note that, while the steady-state reaction appears "simple", behavior on single-crystal planes such as (100) is quite inconsistent with LH models, and the approach to and stability of steady states can be quite complex. We shall describe these phenomena in a later paper.

Acknowledgment. This work was partially supported by NSF under Grant No. DMR8216729.

Registry No. Pt, 7440-06-4; NO, 10102-43-9; CO, 630-08-0.

Measurement of Bromine Removal Rate in the Oscillatory BZ Reaction of Oxalic Acid. Transition from Limit Cycle Oscillations to Excitability via Saddle-Node Infinite Period Bifurcation

Zoltán Noszticzius,* Péter Stirling, and Mária Wittmann

Institute of Physics, Technical University of Budapest, H-1521 Budapest, Hungary

(Received: February 21, 1985; In Final Form: May 28, 1985)

The BZ reaction with oxalic acid substrate is one of the simplest BZ oscillator which oscillates only if the produced bromine is removed by an inert carrier gas. In the present study an electrochemical method is reported to determine k_{BR} , the "rate constant" for bromine removal. Oscillations can be found within a certain interval of the k_{BR} parameter values only. Outside of that range two different excitable states were discovered. Transitions from the oscillatory to the excitable states go via saddle-node infinite period bifurcations. Different types of bifurcations leading to periodic orbits, a two-dimensional phase portrait of an excitable system, and a perturbation technique to reveal that portrait are also discussed.

Introduction

The mechanistic problems of the Belousov-Zhabotinsky (BZ) reactions were reinvestigated in a recent series of papers.¹⁻⁵ Now,

in our opinion, the lack and uncertainty of the rate constants^{1,6} remain a major problem in the numerical simulation of the dif-

(1) Noszticzius, Z.; Farkas, H.; Schelly, Z. A. *J. Chem. Phys.* **1984**, *80*, 6062-6070.

(2) Noszticzius, Z.; Farkas, H.; Schelly, Z. A. *React. Kinet. Catal. Lett.* **1984**, *25*, 305-311.

(3) Noyes, R. M. *J. Chem. Phys.* **1984**, *80*, 6071-6078.